



HAL
open science

Ethaverine and Papaverine Target Cyclin-Dependent Kinase 5 and Inhibit Lung Cancer Cell Proliferation and Migration

Arthur Laure, Chloe Royet, Frédéric Bihel, Blandine Baratte, Stéphane Bach, Marion Peyressatre, May Morris

► **To cite this version:**

Arthur Laure, Chloe Royet, Frédéric Bihel, Blandine Baratte, Stéphane Bach, et al.. Ethaverine and Papaverine Target Cyclin-Dependent Kinase 5 and Inhibit Lung Cancer Cell Proliferation and Migration. ACS Pharmacology & Translational Science, 2024, 7 (5), pp.1377-1385. 10.1021/ac-sptsci.4c00023 . hal-04609131

HAL Id: hal-04609131

<https://hal.science/hal-04609131v1>

Submitted on 13 Nov 2024

HAL is a multi-disciplinary open access archive for the deposit and dissemination of scientific research documents, whether they are published or not. The documents may come from teaching and research institutions in France or abroad, or from public or private research centers.

L'archive ouverte pluridisciplinaire **HAL**, est destinée au dépôt et à la diffusion de documents scientifiques de niveau recherche, publiés ou non, émanant des établissements d'enseignement et de recherche français ou étrangers, des laboratoires publics ou privés.

Ethaverine and Papaverine target CDK5 and inhibit lung cancer cell proliferation and migration.

Arthur Laure¹, Chloé Royet¹, Frederic Bihel², Blandine Baratte^{3,4}, Stéphane Bach^{3,4,5}, Marion Peyressatre¹ and May C. Morris^{1,*}

¹*Institut des Biomolécules Max Mousseron, CNRS, UMR 5247, Université de Montpellier, 1919 Route de Mende, 34293 Montpellier, France* ²*Laboratoire d'Innovation Thérapeutique, IMS, UMR 7200, CNRS, Université de Strasbourg, 67401 Illkirch, France* ³*Sorbonne Université, CNRS, FR2424, Plateforme de criblage KISSf (Kinase Inhibitor Specialized Screening facility), Station Biologique de Roscoff, 29680 Roscoff, France* ⁴*Sorbonne Université, CNRS, UMR8227, Integrative Biology of Marine Models Laboratory (LBI2M), Station Biologique de Roscoff, 29680 Roscoff, France* ⁵*Centre of Excellence for Pharmaceutical Sciences, North-West University, Private Bag X6001, Potchefstroom 2520, South Africa.*

*Correspondence: may.morris@umontpellier.fr

KEYWORDS: CDK5; Kinase; small molecule inhibitor; lung cancer; proliferation; migration

ABSTRACT: CDK5 kinase plays a central role in regulation of neuronal functions and its hyperactivation has been associated with neurodegenerative pathologies and more recently with several human cancers, in particular lung cancer. However ATP-competitive inhibitors targeting CDK5 are poorly selective and suffer limitations, calling for new classes of inhibitors. In a screen for allosteric modulators of CDK5 we identified Ethaverine and closely related derivative Papaverine and showed that they inhibit cell proliferation and migration of non-small cell lung cancer cell lines. Moreover the efficacy of these compounds is significantly enhanced when combined with the ATP-competitive inhibitor Roscovitine, suggesting an additive, dual mechanism of inhibition targeting CDK5. These compounds do not affect CDK5 stability, but thermodenaturation studies performed with A549 cell extracts infer that they interact with CDK5 *in cellulo*. Furthermore, the inhibitory potential of Ethaverine and Papaverine is reduced in A549 cells treated with siRNA directed against CDK5. Taken together our results provide unexpected and novel evidence that Ethaverine and Papaverine constitute promising leads that can be repurposed for targeting CDK5 in lung cancer.

CDK5 kinase is an atypical member of the CDK family, first identified in the brain and historically described as neurospecific due to the localization of its main partner p35/p25^{1,2}. Its neuronal functions have been largely described in various regulatory pathways in the central nervous system (CNS) such as axonal guidance, synaptic transmission, synapse formation, neuronal maturation and migration³. CDK5 dysregulation results in the development of several neurodegenerative diseases, including Alzheimer's, Parkinson's and Huntington's disease, as well as amyotrophic lateral sclerosis⁴. Well beyond its neuronal functions, CDK5 regulates a wide variety of biological functions in non-neuronal tissues such as angiogenesis, myogenesis, vesicular transport, cell adhesion and migration⁵⁻⁷. Overexpression of CDK5 has been reported in many human cancers, including colorectal, head/neck, breast, lung, ovarian, lymphoma, prostatic, sarcoma, myeloma and bladder cancers, thereby emerging as a relevant therapeutic target in oncology⁸⁻¹⁰. In lung cancer in particular, several studies have established an inverse correlation between CDK5/p35 expression in patients with non-small cell lung cancer (NSCLC) and survival, inferring that CDK5 constitutes a prognostic biomarker¹¹. Although the mechanism describing CDK5 regulation and role in lung cancer remains poorly characterized, it has been described as a tumor promoter that enhances cell proliferation and metastasis in lung cancer¹². CDK5 activity, required for migration and

invasion of lung cancer cells was shown to be regulated by Achaete-scute homologue-1 (ASH1)¹³. Taken together these studies provide a strong rationale for targeting CDK5 dysregulation to propose new therapeutic strategies for lung cancer.

Inhibition of CDK5 expression and/or activity reduces lung cancer cell proliferation and metastasis^{12,13}. However there are currently no inhibitors of CDK5 used in the clinic for cancer therapeutics. Indeed most inhibitors developed that target CDK5 such as Roscovitine, Dinaciclib or AT7519, bind to the ATP-pocket and are quite promiscuous, consequently eliciting non-specific and off-target effect related secondary effects⁹. With the aim of developing new generations of CDK5-specific inhibitors, we previously developed a conformational biosensor (CDKCONF5) that discriminates against ATP-competitive inhibitors, which was implemented for screening purposes, thereby enabling successful identification of allosteric CDK5 inhibitors¹⁴. In this study we report on two new compounds, Ethaverine and Papaverine, that we identified through a repositioning approach using CDKCONF5 biosensor, by screening a small library of drugs already characterized for therapeutic indications. The opium alkaloid Papaverine and its ethyl derivative Ethaverine are primarily used as antispasmodic drugs described to inhibit phosphodiesterase PDE4 and PDE10A^{15,16}. We characterized the effect of these two compounds in the

A549 lung cancer cell line and found that they inhibited proliferation and migration. Combination of Ethaverine or Papaverine with the ATP-competitive inhibitor Roscovitine further enhanced inhibition, suggesting a dual mechanism of action involving two different binding sites or populations of CDK5. Moreover, studies in H1299 and PC9 cell lines reveal differences in CDK5 inhibition suggesting a possible dependence on p53. Stability studies did not reveal any major effect of Ethaverine or Papaverine on CDK5 protein levels. However CETSA (cell extract thermodenaturation studies) revealed differences in CDK5 protein thermodenaturation profile, suggesting Ethaverine and Papaverine interact with CDK5 in a cellular context. Finally siRNA-mediated downregulation of CDK5 in A549 cells considerably limits inhibition by Ethaverine and Papaverine, revealing on-target selectivity of these compounds.

This study provides insight into drug repositioning and repurposing of Ethaverine and Papaverine, highlighting a promising and attractive targeting strategy through combination of these newly identified allosteric modulators of CDK5 and ATP-competitive inhibitors of CDK5.

RESULTS

Ethaverine is a conformational modulator of CDK5 that targets CDK5 in A549 cells

The previously described conformational biosensor CDKCONF5¹⁴ was applied to screen a small set of 640 compounds, selected on the basis of structural diversity, and including original scaffolds from F. Bihel's lab (Université de Strasbourg) as well as known pharmacological tools dedicated to drug repurposing. Whilst this assay discriminates against ATP-pocket binding compounds (10 μ M ATP, Roscovitine), compounds that bind CDK5 and induce a conformational changes within the C-lobe and the activation loop are expected to induce significant changes in CDKCONF5 fluorescence. Ethaverine was identified as a hit at 10 μ M in the primary screen with an increase in fluorescence emission of CDKCONF5-Cy3 of 50%, significantly above that of the positive control (the CDK-activating protein CIV), although it is a much smaller compound (**Figure 1A**). To address the specificity of Ethaverine for CDKCONF5, we compared its effect on CDKCONF2 biosensor derived from CDK2, the most closely related kinase to CDK5, and found that at 10 μ M it did not induce any fluorescence enhancement indicative of its selectivity for CDK5 over CDK2 (**Figure 1B**). Ethaverine (**Figure 1C**, R = Et) is not a marketed drug but has been tested in humans, and its very close analog Papaverine (**Figure 1C**, R = Me) has been used for decades as a vasodilator for the treatment of cerebral and peripheral ischemia associated with arterial spasm. Both Papaverine and Ethaverine act by inhibiting phosphodiesterase in smooth muscle cells, which produces increased tissue levels of cyclic adenosine monophosphate and cyclic guanosine 3,5-monophosphate and subsequent relaxation of vascular smooth muscle^{15,16}. As Papaverine and Ethaverine have been tested in humans by oral route without showing any major toxic effect in patients^{23,24}, we considered both compounds for further studies. In order to address whether Ethaverine and Papaverine could inhibit CDK5 activity, we performed kinase activity assays with recombinant CDK5/p25 using R-

Roscovitine as a positive control. These experiments revealed that Ethaverine and Papaverine did not inhibit the catalytic activity of CDK5, irrespective of the ATP concentration (10 and 200 μ M) (**Suppl. Figure S1**), confirming that they do not bind the ATP pocket of CDK5, in line with their identification in a screen which discriminates against ATP-pocket binders, and that they do not tamper with its catalytic function, although they bind and modulate CDK5 conformation.

In order to address whether Ethaverine and Papaverine might target CDK5 in A549 cells we asked whether any of these inhibitors were indeed engaged in target binding in a cellular context. To this aim, we first determined the IC₅₀ of these compounds on A549 cell proliferation after 24h and found that all three compounds had very similar IC₅₀ values: 9.1 \pm 1.9 μ M, 10.6 \pm 5.4 μ M and 8 \pm 3 μ M for Roscovitine, Ethaverine and Papaverine, respectively (**Suppl. Figure S2**). We therefore treated A549 cells with each of these compounds at concentrations equal to their IC₅₀ values and then subjected them to thermodenaturation (CETSA assays) essentially as described in [20], ie following one hour treatment of cells with inhibitors (**Figure 1D**). The relative concentration of CDK5 protein was determined by Western blotting and quantified relative to its concentration at 37°C. Comparison of the thermodenaturation profiles of CDK5 between mock-treated and Roscovitine-treated A549 cells revealed a slight destabilization of CDK5 following Roscovitine treatment, between 41°C and 45°C. Papaverine treatment yielded a CDK5 thermodenaturation profile similar to that of Roscovitine. In contrast, treatment with Ethaverine revealed a different profile tending towards stabilization of CDK5, compared to mock-treated A549 cells. The differences observed in all cases relative to mock-treated cells infer target engagement of CDK5. It should however be noted that statistical variability observed at different temperatures may be associated with incomplete target engagement after only 1hr inhibitor treatment in the CETSA protocol used.

Characterization of the inhibitory potential of Ethaverine and Papaverine on proliferation of A549 lung cancer cell line.

In order to gain further insight into the inhibitory potential of Ethaverine and Papaverine, we compared their efficacy after 24h, 48h and 72h treatment with IC₅₀ concentrations, i.e. 9.1 \pm 1.9 μ M, 10.6 \pm 5.4 μ M and 8 \pm 3 μ M for Roscovitine, Ethaverine and Papaverine, respectively (**Figure 2A-C**, **Table 1**, **Suppl. Table 1**). These kinetic studies revealed that the relative inhibitory efficacy of each compound increased over time with 28 \pm 5,8%, 39 \pm 9,5% and 50 \pm 8,6% inhibition of A549 proliferation after 24h, 48h and 72h treatment with 11 μ M Ethaverine, respectively. Very similar values were obtained following treatment with 8 μ M Papaverine, with 27 \pm 7%, 33 \pm 11,4% and 41 \pm 10,2% inhibition and for 9 μ M Roscovitine, with 32 \pm 6,1%, 47 \pm 6,8% and 51 \pm 9 % inhibition after 24h, 48h, 72h respectively.

To further address the potency of these drugs over time, we asked whether sequential treatment every 24h hours might enhance inhibition observed with a single treatment of A549 cells (**Figure 2A-C**, **Table 1**). Sequential treatment with 9 μ M Roscovitine significantly improved inhibition of proliferation, in-

dicative of a cumulative effect which was already quite noticeable after 48h with $70 \pm 14,9\%$ inhibition compared to $47 \pm 6,8\%$ with a single treatment of Roscovitine, and $74 \pm 12,2\%$ inhibition compared to $51 \pm 9\%$ after 72h. Likewise, sequential treatment with $11 \mu\text{M}$ Ethaverine inhibited proliferation more potently, but less significantly than Roscovitine with $49 \pm 14,5\%$ compared to $39 \pm 9,5\%$ % inhibition of proliferation with a single treatment after 48h, and $60 \pm 10,5\%$ compared to $50 \pm 8,6\%$ inhibition of A549 cell proliferation with a single treatment after 72h. Sequential treatment with $8 \mu\text{M}$ Papaverine exhibited a similar inhibitory profile to Ethaverine at 48h, with $46 \pm 12,6\%$ compared to $33 \pm 11,4\%$ inhibition of proliferation with a single treatment after 48h, but no significant difference compared to single treatment after 72h, with 41% inhibition A549 cell proliferation in both cases.

Since Roscovitine targets the ATP pocket of CDK5, while Ethaverine and its closely related derivative Papaverine were identified as non-ATP pocket binding, allosteric modulators of CDK5 function, we asked to what extent their combination might further potentiate inhibition of A549 cell proliferation (**Figure 2A-C, Table 1**). While treatment of A549 cells with concentrations equal to IC_{50} values of Roscovitine ($9 \mu\text{M}$), Ethaverine ($11 \mu\text{M}$) or Papaverine ($8 \mu\text{M}$) alone inhibited A549 proliferation on average by 30% after 24h, the combination of Roscovitine with Ethaverine or with Papaverine promoted a significant increase of inhibition, with $48 \pm 5,3\%$ and $45 \pm 6\%$ inhibition respectively, after 24h treatment. Likewise Roscovitine/Ethaverine and Roscovitine/Papaverine treatments induced $77 \pm 10,2\%$ and $73 \pm 10,2\%$ inhibition of A549 cell proliferation after 48h treatment as compared to $47 \pm 6,8\%$, $39 \pm 9,5\%$ and $33 \pm 11,4\%$ for Roscovitine, Ethaverine and Papaverine, respectively. After 72h treatment, the combinatorial treatments achieved $88 \pm 8,4\%$ and $82 \pm 11,4\%$ inhibition, as compared to $51 \pm 9\%$, $50 \pm 8,6\%$ and $41 \pm 10,2\%$ for Roscovitine, Ethaverine and Papaverine. Although the combined treatments were not synergistic, the effect of Roscovitine with either Ethaverine or Papaverine was additive, and practically complete at 72h.

Interestingly, when $9 \mu\text{M}$ Roscovitine was combined with $5.5 \mu\text{M}$ ($\frac{1}{2} \text{IC}_{50}$) Ethaverine, similar inhibitory efficacy was observed with $53.8 \pm 9.3\%$, $78.1 \pm 6.3\%$ and $85.2 \pm 2.2\%$ proliferation inhibition after 24h, 48h and 72h, respectively (**Suppl. Figure S3, Suppl. Table 2**). Conversely $9 \mu\text{M}$ Roscovitine combined with $22 \mu\text{M}$ Ethaverine (or 2IC_{50}) did not improve inhibition of proliferation significantly compared to the combination of $9 \mu\text{M}$ Roscovitine with $11 \mu\text{M}$ Ethaverine, with 56.9% , 85.1% and 91.6% inhibition after 24h, 48h and 72h, respectively. Likewise combinatorial treatment of A549 cells with Roscovitine and Papaverine yielded additive effects that enabled complete or almost complete inhibition of A549 proliferation after 48h-72h treatment, with comparable inhibition efficacies whether Papaverine was at $8 \mu\text{M}$, $4 \mu\text{M}$ ($1/2 \text{IC}_{50}$) or $16 \mu\text{M}$ (2IC_{50}) (**Suppl. Figure S4, Suppl. Table 3**).

Finally, sequential treatment of A549 cells with combinations of Roscovitine and either Ethaverine or Papaverine, only induced a very slight increase in inhibition compared to a single treatment of these drug combinations, indicating that complete inhibition was essentially achieved with a single combination of the ATP-competitive inhibitor and an allosteric inhibitor of CDK5 after 48h and 72h. Roscovitine/Ethaverine sequential treatment promoted $85 \pm 4,3\%$ and $92 \pm 8,6\%$ inhibition after 48h and 72h, respectively, as compared to $77 \pm 10,2\%$ and $88 \pm$

$8,4\%$ for Roscovitine/Ethaverine single treatment. Roscovitine/Papaverine sequential treatment induced $84 \pm 5,2\%$ and $90 \pm 3,2\%$ inhibition after 48h and 72h, respectively as compared to $77 \pm 9,9\%$ and $88 \pm 11,4\%$ for a single treatment (**Figure 2A-C, Table 2, Suppl. Table 1**).

Taken together the differences observed between Roscovitine, Ethaverine and Papaverine when A549 cells were treated sequentially with these drugs, as well as the increased inhibitory efficacy observed with combinations of Roscovitine with Ethaverine or Papaverine highlight both differences in inhibitory potential over time and point to different mechanisms of action between Roscovitine, Ethaverine and Papaverine.

Roscovitine, Ethaverine and Papaverine exhibit different inhibitory profiles in NSCLC cell lines with different p53 status

An interdependent regulatory mechanism has been described between CDK5 and p53²⁵. Since A549 cells are p53 +/+, we asked whether Ethaverine and Papaverine exhibited the same inhibitory efficacy in other NSCLC cell lines, in which p53 was either deleted or mutated. To this aim, the H1299 cell line which is p53^{-/-} and the PC9 cell line which harbours the p53 R248Q mutation were treated with Roscovitine, Ethaverine and Papaverine²⁶. While the efficacy of Ethaverine and Papaverine in H1299 and PC9 was quite similar to that observed in A549 cells with an average 30% inhibition after 24h treatment, Roscovitine was much less efficient with only $14 \pm 12,3\%$ and $23 \pm 12\%$ inhibition in H1299 and PC9, respectively, compared to $32 \pm 6,1\%$ in A549 cells (**Figure 3, Table 2, Suppl. Table 4**). In line with this reduced efficacy of Roscovitine in H1299 cells we observed that the combined treatment of Roscovitine with either Ethaverine or Papaverine only inhibited H1299 cell proliferation by $36 \pm 11,3\%$ and $35 \pm 13,8\%$, respectively, after 24h, compared to $48 \pm 5,3\%$ and $45 \pm 6\%$ inhibition in A549 cells. PC9 cell proliferation was still inhibited to the same extent as A549 cells, with $45 \pm 15\%$ and $41 \pm 17,2\%$ inhibition after 24h treatment. Comparison of the inhibitory efficacies of these drugs after 48h again revealed much lower efficacy of Roscovitine in H1299 and PC9 cells with $27 \pm 7,2\%$ and $28 \pm 14,1\%$ inhibition, respectively compared to $47 \pm 6,8\%$ inhibition of A549 cells, whereas Ethaverine and Papaverine exhibited very similar inhibitory efficacy in all three cell lines, with an average 40% inhibition of Ethaverine and 33% inhibition of Papaverine. Again, in line with the reduced efficacy of Roscovitine, combined treatments lead to lower inhibition of proliferation of the H1299 and PC9 cell lines, with $61 \pm 7,3\%$ and $69 \pm 5,1\%$ inhibition following combined treatment with Roscovitine and Ethaverine in H1299 and PC9 cell lines compared to $77 \pm 10,2\%$ inhibition in A549 cell lines; $56 \pm 2,9\%$ and $62 \pm 21,5\%$ inhibition following combined treatment with Roscovitine and Papaverine in H1299 and PC9 cell lines compared to $73 \pm 9,9\%$ inhibition in A549 cells. The reduced efficacy of Roscovitine in H1299 and PC9 cells was observed after 72 hours with $32 \pm 8,7\%$ and $14 \pm 6,3\%$ inhibition in H1299 and PC9 cells, compared to $51 \pm 9\%$ inhibition in A549 cells. However treatment with Ethaverine and Papaverine exhibited different trends, the former inducing $49 \pm 9,2\%$, $40 \pm 5,7\%$ and $50 \pm 9\%$ inhibition of H1299, PC9 and A549 cells, respectively, whilst Papaverine induced $44 \pm 8,7\%$ and $19 \pm 4,2\%$ inhibition in H1299 and PC9 cells, compared to $41 \pm 10,2\%$ inhibition in A549 cells. Again, combined treatments with Roscovitine/ Ethaverine and with Roscovitine / Papaverine were slightly less efficient in H1299 and PC9 cells, with $76 \pm 5,3\%$ and $72 \pm 6,7\%$ inhibition in

H1299 cells, $72 \pm 5,3\%$ and $61 \pm 9,8\%$ in PC9 cells, compared to $88 \pm 8,4\%$ and $82 \pm 11,4\%$ inhibition in A549 cells.

To address whether the differences in response between these three cell lines, were associated with differences in IC₅₀ values for Roscovitine, Ethaverine and Papaverine we determined the IC₅₀ values for each drug in PC9 and H1299 cell lines (**Suppl. Figure S2**). IC₅₀ values for PC9 cells are $19,8 \pm 1,6$ for Roscovitine, $24,7 \pm 7,6$ for Ethaverine $23,4 \pm 2,4$ for Papaverine. In H1299 cells, IC₅₀ values are $16,6 \pm 4,8$ for Roscovitine, $20,3 \pm 7,3$ for Ethaverine and $18,5 \pm 3$ for Papaverine. Furthermore statistical analysis revealed that the main and most significant differences in inhibitory efficacy between A549 cells and the two other cell lines were observed for Roscovitine at 24h, 48h and 72h, as well as for Ethaverine in PC9 cells, and Papaverine in PC9 cells at 24h and 72h (**Suppl. Figure S5**). Whilst differences in the IC₅₀ for Roscovitine between A549 and the two other cell lines can explain the lower inhibitory efficacy obtained in our experiments with treatments using the IC₅₀ concentrations determined in A549 cells, they cannot explain the greater inhibitory efficacy in PC9 cells for Ethaverine and Papaverine, since the IC₅₀ values for these two compounds are 2-3 fold greater than those in A549 cells. Likewise it is quite surprising to observe similar inhibitory efficacies of H1299 cells in our experiments for Ethaverine and Papaverine, since their IC₅₀ values are approximately 2- fold greater than those in A549 cells.

Taken together, these results raise the question of CDK5 inhibition relative to p53 status. They reveal that the ATP-competitive inhibitor Roscovitine and the allosteric modulators Ethaverine and Papaverine still inhibit CDK5 efficiently in an additive fashion when combined. However they also show that Ethaverine and Papaverine are more robust inhibitors than Roscovitine, since efficacy of the latter is reduced when wild-type p53 is not expressed, whereas Ethaverine and Papaverine efficacy is essentially identical, irrespective of p53 status. Since a CDK5 has been shown to stabilize and promote p53 activation, thereby contributing to neuronal cell death²⁵, we further investigated whether Ethaverine might somehow impact p53 expression and found that p53 levels increase following treatment of A549 cells with $11 \mu\text{M}$ Ethaverine for 48h (**Suppl. Figure S6**).

Knockdown of CDK5 with siRNA combined with drugs targeting CDK5 reduces inhibition of A549 cell proliferation by Ethaverine.

To address the selectivity of CDK5 inhibition by Ethaverine and Roscovitine, we finally asked whether these drugs might still be effective on inhibition of A549 proliferation, following downregulation of CDK5 protein by siRNA treatment. To this aim, we first established experimental conditions to achieve a significant knockdown of CDK5 protein (40-50%) 24h following treatment of A549 cells with 100nM or 200nM siRNA complexed with the cell-penetrating peptide CADY as previously described¹⁹ (**Figure 4A**). siRNA directed against CDK5 induced a transient inhibition of A549 cell proliferation when cells were treated once, i.e. 26% after 24h, 19% after 48h (**Figure 4B, Table 3**). However a second siRNA treatment 24h after the first (siRNA 1+2) elicited a greater inhibition of CDK5 proliferation, i.e. 51% compared to 19% inhibition 48h after initial treatment, and a third boost of siRNA led to 62% inhibition 72h after initial treatment. When cells were treated with Roscovitine/Ethaverine combination (IC₅₀ concentration of each), 24h after A549 cells had been treated once with siRNA directed against CDK5, and incubated for another 24h (ie 48h total

siRNA + Rosco/Etha), there was an additional 25% inhibition of proliferation, relative to A549 cells treated once with siRNA alone, inferring that there was still plenty of active CDK5 to be inhibited by Roscovitine/Ethaverine. In contrast, no additional inhibition of A549 cell proliferation was observed when cells were treated with Roscovitine/Ethaverine following a double treatment with siRNA (siRNA1+2 + Rosco/Etha) relative to cells treated twice with siRNA alone (siRNA 1+2) 48h after the first treatment, with $42\% \pm 5,2$ and $51\% \pm 1,7$ inhibition respectively. Likewise, cells treated with a combination of Roscovitine/Ethaverine following daily treatment with siRNA (siRNA 1+2+3 + Rosco/Etha) with $66\% \pm 2,7$ inhibition of proliferation after 72h did not exhibit any additional inhibition, compared to cells treated with Roscovitine/Ethaverine alone for 72h, with $66\% \pm 1,5$ inhibition of proliferation, and cells treated three times with siRNA directed against CDK5 (siRNA 1+2+3) with $62\% \pm 5,1$ inhibition. Taken together these results infer that once CDK5 protein levels are significantly downregulated there is no further inhibition possible, in line with the selectivity of Ethaverine for CDK5. Whilst CDK5 levels are reduced by 40-50% following a single siRNA treatment after 24h, CDK5 levels increase again significantly after 48h, implying that it is resynthesized following the 24h knockdown (**Figure 4C**). In contrast a triple siRNA treatment leads to 71% CDK5 knockdown relative to mock at 72h. This significant knockdown of CDK5 protein is in line with both the significant inhibition of A549 cell proliferation after 72h and also explains why Roscovitine and Ethaverine co-treatment have no further effect on cell proliferation of the triple siRNA treated-cells.

Timelapse studies of kinetics of cell division inhibition and migration

To gain further insight into the kinetics and mechanism leading to inhibition of cell proliferation, we performed time-lapse imaging on A549 cells treated with Roscovitine, Ethaverine or Papaverine alone at their IC₅₀ value, or in combination and counted the number of cell divisions following each treatment over the first 24h, then during the interval between 24h and 48h (**Figure 5 and Suppl. Tables S5 & S6**). These studies revealed that inhibition of cell division was more effective during the second 24h interval for Ethaverine and Papaverine, whereas the average number of cell divisions remained similar for cells treated with Roscovitine during the first 24h post-treatment and during the interval from 24h-48h. Combinations of either Ethaverine or Papaverine with Roscovitine were already quite effective during the first 24h and cell division remained inhibited up to 48h.

We further performed FACS analysis following propidium iodide staining of A549 cells treated with Roscovitine or Ethaverine for 48h, but did not observe any major effect on the 2N or 4N content of cells (**Suppl. Figure S7**). Western Blots of cyclin A, cyclin B, phospho-cyclin B, phospho-Histone H3, revealed a net increase in cyclin A levels, a decrease in cyclin B1 levels, and slight increase in phospho-cyclin B1 and phospho-Histone H1 (**Suppl. Figure S8**). We finally addressed whether apoptosis was induced and performed Western blots of cleaved caspase 3, caspase 8, caspase 9 and cleaved PARP after 48h treatment with $10 \mu\text{M}$ ethaverine. Quantification of their expression levels relative to GAPDH revealed an increase in caspase 8 and 3, but no significant increase in cleaved caspase 9 or PARP (**Suppl. Figure S9**).

Since CDK5 has been reported for its function in cell migration²⁷⁻³¹, we further asked whether Ethaverine and Papaverine

might affect this process in addition to cell division. To this aim a standard “scratch test” was performed on A549 cells grown to confluence by inflicting a wound and monitoring the kinetics of recolonization over 24h and 48h (**Figure 6, Suppl. Figure S10, and Suppl. Tables S7 & S8**). Mock-treated cells recolonized the wound surface quite rapidly, essentially during the first 24h. Roscovitine treatment reduced migration of cells to recolonize the wound by approximately half during the first 24h but, after this time, exhibited similar kinetics to mock-treated cells. In contrast, Ethaverine and Papaverine exhibited a very similar behaviour to mock-treated cells over the first 24h, but then completely stopped migrating between 24h and 48h. Combined treatment of Roscovitine and either Ethaverine or Papaverine affected migration similarly to Roscovitine during the first 24h, and almost completely inhibited migration during the next 24h, following a similar trend to cells treated with Ethaverine and Papaverine alone. Taken together these results again point to distinct mechanisms of action for Roscovitine and Ethaverine/Papaverine, the former affecting migration at an early stage, the latter 24h-48h after treatment, whether alone or in combination.

DISCUSSION

Lung cancers and in particular NSCLC currently suffer from a lack of efficient targeted therapies. CDK5 hyperactivity has been reported in human lung cancers and constitutes an attractive therapeutic target^{11,12}. Although a wide variety of CDK5 inhibitors are available, including compounds targeting the ATP-pocket such as Roscovitine, Purvalanol, Dinaciclib and AT7519 and peptides targeting the CDK5/p25 interface⁹, the former lack selectivity, resulting in a variety of undesirable secondary effects, the latter are characterized by penetration and bioavailability issues that limit their development for clinical use.

In this study we report on the identification of Ethaverine and its closely related derivative Papaverine, which we have identified as allosteric modulators of CDK5 using a conformational CDK5 biosensor¹⁴. Since Ethaverine and Papaverine are well established PDE inhibitors^{15,16}, it was quite surprising to identify these compounds repositioned as CDK5 binders and modulators of its conformation. Our *in vitro* assays with CDKCONF5/CDKCONF2 indicate that these compounds indeed bind selectively to CDK5 and our CETSA studies suggest that Ethaverine and Papaverine interact physically with CDK5 in A549 cells, since its thermodenaturation profile was affected following treatment with these inhibitors.

We demonstrate that Ethaverine and Papaverine target CDK5 function in cell proliferation and migration, thereby offering alternatives to conventional ATP-competitive inhibitors. We have shown that these compounds inhibit proliferation of the A549 lung cancer cell line, with moderate efficiency, comparable to that of Roscovitine. However, we have also found that their combination with the ATP-competitive inhibitor Roscovitine leads to essentially complete inhibition of proliferation, suggesting that Ethaverine/Papaverine and Roscovitine may simultaneously target CDK5 through different binding pockets, or alternatively target different populations of CDK5. In fact the differences observed between Roscovitine, Ethaverine and Papaverine throughout this study, whether in proliferation assays, following sequential treatments, in different cell lines, and in time-lapse imaging studies of cell division and migration, point

to different mechanisms of action between these newly-identified allosteric modulators of CDK5 and Roscovitine. Last but not least, our finding that Ethaverine and Papaverine are more robust inhibitors than Roscovitine in cells that do not express wild-type p53, underscores their therapeutic attractivity in cancers that lack p53 or express mutant forms such as R248Q.

We have previously shown that combination strategies using kinase inhibitors that target CDKs through different mechanisms of action constitute promising therapeutic strategies enabling to achieve complete inhibition³². In this study we demonstrate that combination of Ethaverine or Papaverine with the ATP-competitive inhibitor Roscovitine induce an additive and efficient inhibition of NSCLC cell proliferation. Hence the combination of these different compounds is an attractive strategy for anti-cancer therapeutics that offers several advantages a single drug cannot achieve. ATP-competitive kinase inhibitors are notorious for their promiscuity as well as their ability to induce resistance, essentially associated with mutations in the ATP-binding pocket or compensation mechanisms^{33,34}. In contrast, allosteric modulators are believed to achieve greater selectivity by targeting pockets and interfaces which are not conserved in different kinases and little if any resistance³⁵⁻³⁸.

CONCLUSIONS

This study provides insight into drug repositioning and repurposing of Ethaverine and Papaverine and highlights a promising and attractive targeting strategy through combination of these newly identified allosteric modulators of CDK5 and ATP-competitive inhibitors of CDK5. Our strategy emphasizes the originality and relevance of a conformational biosensor to identify allosteric modulators of kinase function, providing means to screen for “old drugs” which may be repurposed for cancer therapeutics. It also reveals that combinatorial treatment with allosteric drugs and ATP-competitive inhibitors, can enhance inhibition of the same target, thereby reducing the overall concentration of drugs required for treatment and potentially preventing emergence of resistance. The efficient inhibition of lung cancer cell proliferation and migration by Ethaverine/Papaverine and Roscovitine suggests CDK5 targeting could involve either two distinct binding sites or two conformationally distinct populations of CDK5. The combination of compounds targeting the same kinase with different mechanisms of action can be expected to tamper with distinct functions or signalling processes simultaneously and therefore constitutes an efficient therapeutic strategy. Moreover combination of FDA-approved inhibitors targeting other kinases currently used in NSCLC such as Erlotinib, Gefinitib or Crizotinib, or CDK4/6 inhibitors Abemaciclib, Palbociclib and Ribociclib, might potentially also be combined with Ethaverine or Papaverine.

FIGURES

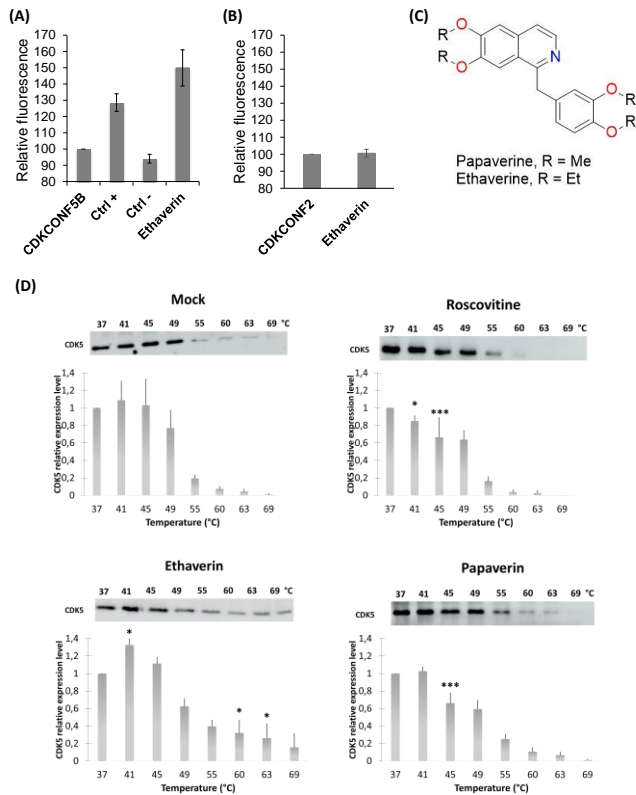


Figure 1. Identification of Ethaverine as an allosteric modulator of CDK5. (A) Fluorescence-based screen for allosteric modulators of CDK5 with the CDKCONF5-Cy3 biosensor led to identification of Ethaverine; Ctrl+ is 200 nM of the CDK-activating protein CIV and Ctrl- corresponds to 10 μ M ATP as described in [14]. (B) Fluorescence-based assay with CDKCONF2 biosensor as described in [17]: Ethaverine does not modulate the fluorescence of CDKCONF2-Cy3 (C) Chemical structures of Ethaverine and Papaverine; Ethaverine bears four ethyl groups (R=Et), whereas Papaverine bears four methyl groups (R=Me) (D) Thermodenaturation profiles of CDK5 from lysates of A549 cells, following treatment with Roscovitine, Ethaverine or Papaverine at their IC₅₀ concentration. Statistical significance : * $p < 0.0332$, ** $p < 0.0021$.

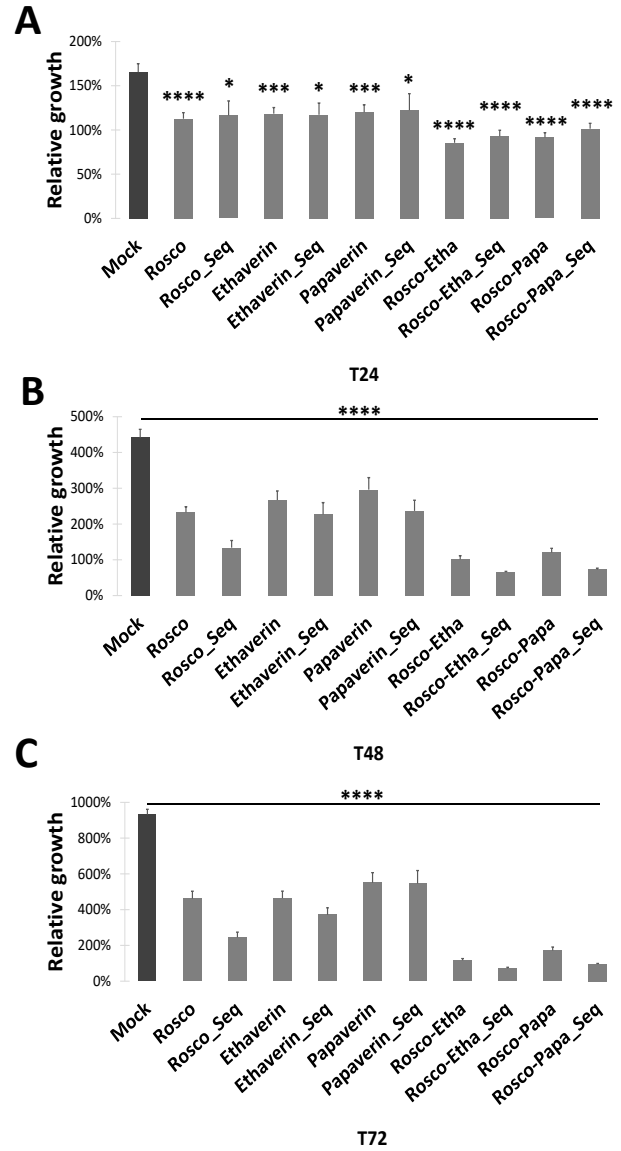


Figure 2. Papaverine and Ethaverine inhibit proliferation of A549 cells. Proliferation Assays performed on A549 cells with 9 μ M Roscovitine, 11 μ M Ethaverine or 8 μ M Papaverine alone, in combination, or following sequential addition (A) after 24h (B) after 48h (C) after 72h. Histograms represent mean relative growth of A549 cells as determined by crystal violet absorbance measured at 595nm \pm SEM relative to their absorbance at T0 in three independent experiments.

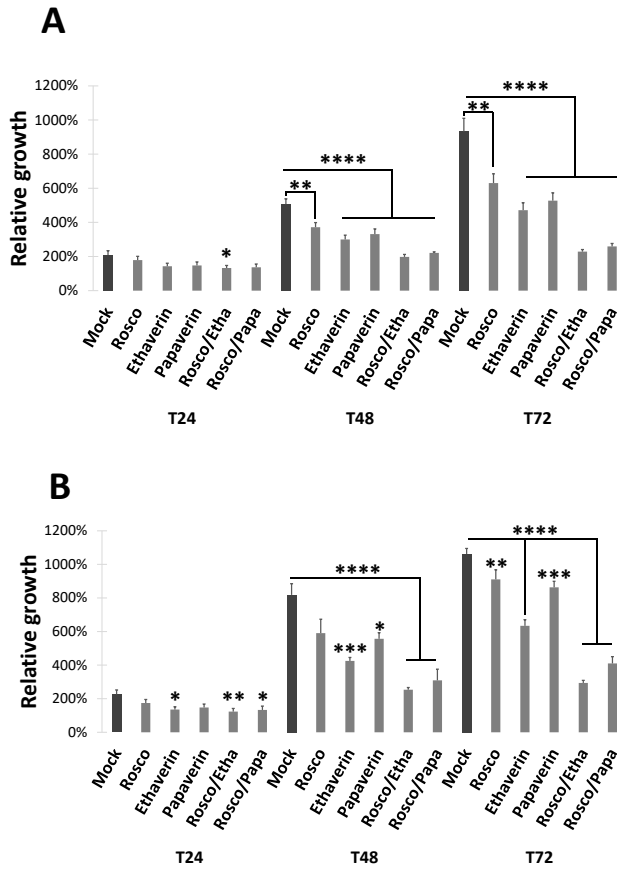


Figure 3. Papaverine and Ethaverine inhibit proliferation of H1299 and PC9 cells. Proliferation assays performed (A) on H1299 cells (B) on PC9 with 9 μ M Roscovitine, 11 μ M Ethaverine or 8 μ M Papaverine alone, or in combination as described for A549 cells in Figure 2. Histograms represent mean relative growth of cells as determined by crystal violet absorbance measured at 595nm \pm SEM relative to their absorbance at T0 in three independent experiments. Statistical significance: * $p < 0.0332$, ** $p < 0.0021$, *** $p < 0.002$ and **** $p < 0.0001$.

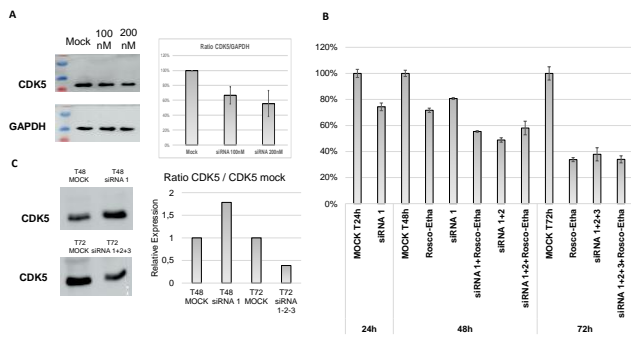


Figure 4. Knockdown of CDK5 with siRNA combined with Ethaverine and Papaverine treatments in A549 cells. (A) A549 cells were treated with 100nM or 200nM siRNA targeting CDK5. Representative Western blots of CDK5 and GAPDH and quantification of relative CDK5 protein levels in 20 μ g lysates from mock and siRNA-treated A549 cells from three independent experiments after 24h treatment. (B) Crystal violet proliferation assay of mock-treated A549 cells and A549 cells treated with 100nM siRNA targeting CDK5 one, twice or three times (siRNA 1, 1+2 or 1+2+3), after 24h, 48h and 72h alone or combined with Roscovitine / Ethaverine treatment (24h after the first siRNA treatment). (C) Western

blot of CDK5 levels 48h after the first siRNA treatment and after 72h with three siRNA treatments, and their respective mock treated cells at 24h and at 72h; quantification of CDK5 levels in treated cells relative to that in mock-treated cells at the same time points.

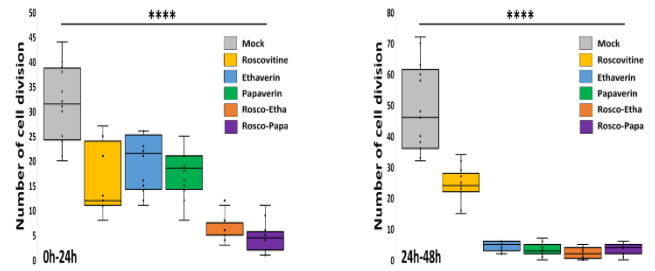


Figure 5. Time-lapse imaging of A549 cells treated with Ethaverine and Papaverine reveals differences in cell division A549 cells were either mock-treated or treated with Roscovitine, Ethaverine, Papaverine at their IC₅₀ concentration or co-treated with Roscovitine/Ethaverine or Roscovitine/Papaverine and timelapse microscopy was performed (a) for the first 24h hours following treatment and (b) between 24h and 48h post-treatment. The total number of cell divisions were counted from images acquired in three independent experiments and six different fields per experiment and are represented as box plots. Statistical significance: **** $p < 0.0001$

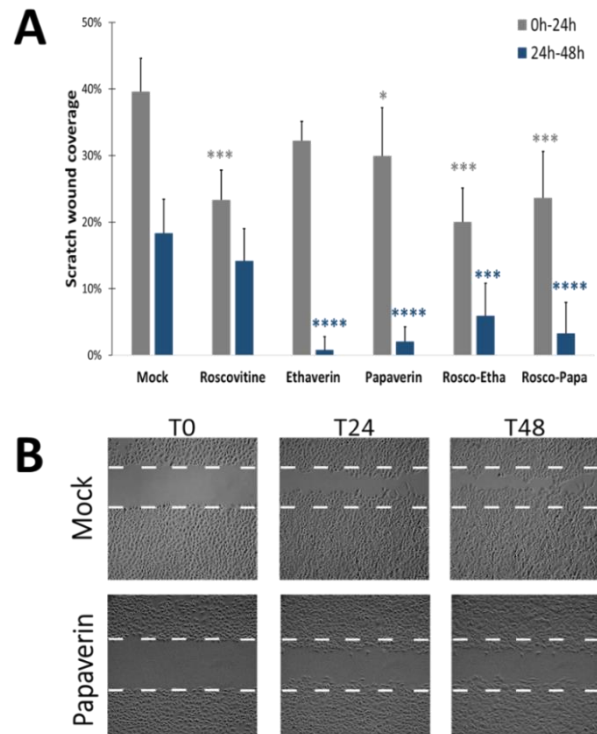


Figure 6. Time-lapse imaging of A549 cells treated with Ethaverine and Papaverine reveals differences in cell migration A549 cells were either mock-treated or treated with Roscovitine, Ethaverine, Papaverine at their IC₅₀ concentration or co-treated with Roscovitine/Ethaverine or Roscovitine/Papaverine and time-lapse microscopy was performed for the first 24h hours following treatment and between 24h and 48h post-treatment. (a) The ability of cells to recolonize the wounded area in the well where a scratch had been made is represented as the percentage of surface coverage relative to T0 (scratch) Histogram values represent the mean \pm SD from five different fields in each of two independent experiments.

Statistical significance: * $p < 0.0332$, ** $p < 0.0021$, *** $p < 0.002$ and **** $p < 0.0001$. (c) micrographs of mock-treated and Ethaverine treated cells (b) Representative micrographs of mock-treated cells and cells treated with Papaverine.

ASSOCIATED CONTENT

Supporting Information. A brief statement in nonsentence format listing the contents of material supplied as Supporting Information should be included, ending with “This material is available free of charge via the Internet at <http://pubs.acs.org>.” For instructions on what should be included in the Supporting Information as well as how to prepare this material for publication, refer to the journal’s Instructions for Authors.

Supplementary Materials: The following are available online at www.mdpi.com/xxx/s1, Figure S1. CDK5/p25 Kinase Activity Inhibition by Roscovitine, Ethaverine and Papaverine, Figure S2. Determination of IC50 values for Roscovitine, Ethaverine and Papaverine in A549 cells, Figure S3. A549 proliferation assay following treatment with Ethaverine and Roscovitine/Ethaverine, Figure S4. A549 proliferation assay following treatment with Papaverine and Roscovitine/Papaverine, Figure S5. Statistical differences between cell lines following treatment with drugs, Figure S6. Western blotting of p53 levels in A549 cells treated with Ethaverine, Figure S7 - FACS Analysis of A549 cells treated with Roscovitine, Ethaverine and Papaverine, Figure S8 Western Blotting of cell cycle markers, Figure S9. Western Blotting of apoptosis markers, Figure S10. Time-lapse imaging of A549 cell migration, Table S1. Relative proliferation of A549 cells, Table S2. Relative proliferation and inhibition of A549 cells, Table S3. Relative proliferation of A549 cells.

AUTHOR INFORMATION

Corresponding Author

* Dr. May C. MORRIS, Email: may.morris@umontpellier.fr

Author Contributions

The manuscript was written through contributions of all authors. / All authors have given approval to the final version of the manuscript.

Funding Sources

This work was funded by the LABEX Medalis (ANR-10-LABX-0034) and by the Interdisciplinary Thematic Institute IMS (Institut du Médicament de Strasbourg), as part of the ITI 2021-2028 program of the University of Strasbourg, CNRS and Inserm supported by IdEx Unistra (ANR-10-IDEX-0002) and SFRI (STRAT*US project, ANR-20-SFRI-0012) under the framework of the French Investments for the Future Program. A.L. received a fellowship from the Princely Government of Monaco.

ACKNOWLEDGMENT

We further acknowledge continuous support from the CNRS (Centre National de la Recherche Scientifique). We acknowledge the MRI imaging facility (CRBM Montpellier, FRANCE), a member of the national infrastructure France-BioImaging and Euro-BioImaging. The authors also thank the Cancéropôle Grand Ouest (3MC network—Marine Molecules, Metabolism and Cancer), GIS IBiSA (Infrastructures en Biologie Santé et Agronomie) and Biogenouest (Western France life science and environment core facility network

supported by the Conseil Régional de Bretagne) for supporting the KISSf screening facility (FR2424, CNRS and Sorbonne Université), Roscoff, France.

ABBREVIATIONS

CDK, cyclin-dependent kinase; NSCLC, non-small cell lung cancer.

REFERENCES

- (1) Hellmich, M.R.; Pant, H.C.; Wada, E.; Battey, J.F. Neuronal cdc2-like kinase: a cdc2-related protein kinase with predominantly neuronal expression. *Proc. Natl. Acad. Sci. U.S.A.* **1992**, *89*, 10867-71, doi:10.1073/pnas.89.22.10867.
- (2) Tsai, L.-H.; Delalle, I.; Caviness, V.S.; Chae, T.; Harlow, E. p35 is a neural-specific regulatory subunit of cyclin-dependent kinase 5. *Nature* **1994**, *371*, 419-423, doi:10.1038/371419a0.
- (3) Dhavan, R.; Tsai, L.H. A decade of CDK5. *Nat. Rev. Mol. Cell Biol.* **2001**, *2*, 749-749, doi:10.1038/35096019.
- (4) Cheung, Z.H.; Ip, N.Y. CDK5: A multifaceted kinase in neurodegenerative diseases. *Trends Cell Biol.* **2012**, *22*, 1696175, doi:10.1016/j.tcb.2011.11.003.
- (5) Contreras-Vallejos, E.; Utreras, E.; Gonzales-Billault, C. Going out of the brain: Non-nervous system physiological and pathological functions of Cdk5. *Cell Signal.* **2012**, *24*, 44-52, doi:10.1016/j.cellsig.2011.08.022.
- (6) Sharma, S.; Sicinski, P. A kinase of many talents: Non-neuronal functions of CDK5 in development and disease. *Open Biol.* **2020**, *10*, doi:10/1098/rsob.190287.
- (7) Rosales, J.L.; Lee, K.Y. Extraneuronal roles of cyclin-dependent kinase 5. *BioEssays* **2006**, *28*, 1023-1034, doi:10.1002/bies.20473.
- (8) Pozo, K.; Bibb, J.A. The Emerging Role of Cdk5 in Cancer. *Trends Cancer* **2016**, *63*, 217-232, doi:10.1002/hep.28274.Integrin.
- (9) Peyressatre, M.; Prével, C.; Pellerano, M.; Morris, M.C. Targeting cyclin-dependent kinases in human cancers: From small molecules to peptide inhibitors. *Cancer (Basel)*. **2015**, *7*, 179-237, doi:10.3390/cancers7010179.
- (10) Shupp, A.; Casimiro, M.C.; Restell, R.G. Biological functions of CDK5 and potential CDK5 targeted clinical treatments. *Oncotarget* **2017**, *8*, 17373-17382, doi:10.18632/oncotarget.14538.
- (11) Liu, J.L.; Wang, X.Y.; Huang, B.X.; Zhu, F.; Zhang, R.G.; Wu, G. Expression of CDK5/p35 in resected patients with non-small cell lung cancer: Relation to prognosis. *Med. Oncol.* **2011**, *28*, 673-678, doi:10.1007/s12032-010-9519-7.
- (12) Zeng, J.; Xie, S.; Liu, Y.; Shen, C.; Song, X.; Zhou, G.L.; Wang, C. CDK5 functions as a tumor promoter in human lung cancer. *J. Cancer* **2018**, *9*, 3950-3961, doi:10.7150/jca.25967.
- (13) Demelash, A.; Rudrabhatla, P.; Pant, H.C.; Wang, X.; Amin, N.D.; McWhite, C.D.; Naizhen, X.; Linnoila, R.I. Achaete-scute homologue-1 (ASH)

- stimulates migration of lung cancer cells through Cdk5/p35 pathway. *Mol. Biol. Cell* **2012**, *23*, 2856–2866, doi: 10.1091/mbc.E10-12-1010.
- (14) Peyressatre, M.; Arama, D.P.; Laure, A.; González-Vera, J.A.; Pellerano, M.; Masurier, N.; Morris, M.C. Identification of Quinazolinone Analogs Targeting CDK5 Kinase Activity and Glioblastoma Cell Proliferation. *Front. Chem.* **2020**, *8*, 1–12, doi:10.3389/fchem.2020.00691.
 - (15) Bihel, F.J.J.; Justiniano, H.; Schmitt, M.; Hellal, M.; Ibrahim, M.A.; Lugnier, C.; Bourguignon, J.J. New PDE4 inhibitors based on pharmacophoric similarity between Papaverine and tofisopam. *Bioorganic Med. Chem. Lett.* **2011**, *21*, 6567–6572, doi:10.1016/j.bmcl.2011.08.036.
 - (16) Siuciak, J.A.; Chapin, D.S.; Harms, J.F.; Lebel, L.A.; McCarthy, S.A.; Chambers, L.; Shrikhande, A.; Wong, S.; Menniti, F.S.; Schmidt, C.J. Inhibition of the striatum-enriched phosphodiesterase PDE10A: A novel approach to the treatment of psychosis. *Neuropharmacology* **2006**, *51*, 386–396, doi:10.1016/j.neuropharm.2006.04.013.
 - (17) Pellerano, M.; Tcherniuk, S.; Perals, C.; Ngoc Van, T.N.; Garcin, E.; Mahuteau-Betzer, F.; Teulade-Fichou, M.P.; Morris, M.C. Targeting Conformational Activation of CDK2 Kinase. *Biotechnol. J.* **2017**, *12*, doi:10.1002/biot.201600531.
 - (18) Peyressatre, M.; Laure, A.; Pellerano, M.; Boukhadadoui, H.; Soussi, I.; Morris, M.C. Fluorescent Biosensor of CDK5 Kinase Activity in Glioblastoma Cell Extracts and Living Cells. *Biotechnol. J.* **2020**, *15*, 1–24, doi:10.1002/biot.201900474.
 - (19) Crombez L, Aldrian-Herrada G, Konate K, Nguyen QN, McMaster GK, Brasseur R, Heitz F, Divita G. A new potent secondary amphipathic cell-penetrating peptide for siRNA delivery into mammalian cells. *Mol Ther.* **2009**, *17*, 95–103. doi: 10.1038/mt.2008.215. Epub 2008 Oct 28
 - (20) Miettinen, T.P.; Peltier, J.; Härtlova, A.; Gierliński, M.; Jansen, V.M.; Trost, M.; Björklund, M. Thermal proteome profiling of breast cancer cells reveals proteasomal activation by CDK 4/6 inhibitor palbociclib. *EMBO J.* **2018**, *37*, 1–19, doi:10.15252/embj.201798359.
 - (21) Liang, C.C.; Park, A.Y.; Guan, J.L. In vitro scratch assay: A convenient and inexpensive method for analysis of cell migration in vitro. *Nat. Protoc.* **2007**, *2*, 329–333, doi:10.1038/nprot.2007.30.
 - (22) Suarez-Arnedo, A.; Figueroa, F.T.; Clavijo, C.; Arbeláez, P.; Cruz, J.C.; Muñoz-Camargo, C. An image J plugin for the high throughput image analysis of in vitro scratch wound healing assays. *PLoS One* **2020**, *15*, 1–14, doi:10.1371/journal.pone.0232565.
 - (23) Oswald WJ, Baeder DH. Pharmacology of ethaverine HC1: human and animal studies. *South Med J.* **1975** *68*, 1481–4. doi: 10.1097/00007611-197512000-00007.
 - (24) Ritschel WA, Hammer GV. Pharmacokinetics of papaverine in man. *Int J Clin Pharmacol Biopharm.* **1977**, *15*, 227–8. doi: 10.1097/00007611-197512000-00007.
 - (25) Lee, J.H.; Kim, H.S.; Lee, S.J.; Kim, K.T. Stabilization and activation of p53 induced by Cdk5 contributes to neuronal cell death. *J. Cell Sci.* **2007**, *120*, 2259–2271, doi:10.1242/jcs.03468.
 - (26) Pellerano, M.; Naud-Martin, D.; Mahuteau-Betzer, F.; Morille, M.; Morris, M.C. Fluorescent Biosensor for Detection of the R248Q Aggregation-Prone Mutant of p53. *ChemBioChem* **2019**, *20*, 605–613, doi:10.1002/cbic.201800531.
 - (27) Liebl, J.; Weitensteiner, S.B.; Vereb, G.; Takács, L.; Fürst, R.; Vollmar, A.M.; Zahler, S. Cyclin-dependent kinase 5 regulates endothelial cell migration and angiogenesis. *J. Biol. Chem.* **2010**, *285*, 35932–35943, doi:10.1074/jbc.M110.126177.
 - (28) Gao, C.; Negash, S.; Guo, H.T.; Ledee, D.; Wang, H.S.; Zelenka, P. CDK5 regulates cell adhesion and migration in corneal epithelial cells. *Mol Cancer Res* **2002**, *1*, 12–24.
 - (29) Ohshima, T.; Gilmore, E.C.; Longenecker, G.; Jacobowitz, D.M.; Brady, R.O.; Herrup, K.; Kulkarni, a B. Migration defects of cdk5(-/-) neurons in the developing cerebellum is cell autonomous. *J. Neurosci.* **1999**, *19*, 6017–6026, doi: 10.1523/JNEUROSCI.19-14-06017.1999.
 - (30) Strock CJ, Park JI, Nakakura EK, Bova GS, Isaacs JT, Ball DW, Nelkin BD. Cyclin-dependent kinase 5 activity controls cell motility and metastatic potential of prostate cancer cells. *Cancer Res.* **2006**, *66*, 7509–7515, doi: 10.1158/0008-5472.CAN-05-3048.
 - (31) Bisht S, Nolting J, Schütte U, Haarmann J, Jain P, Shah D, Brossart P, Flaherty P, Feldmann G. Cyclin-Dependent Kinase 5 (CDK5) Controls Melanoma Cell Motility, Invasiveness, and Metastatic Spread-Identification of a Promising Novel therapeutic target. *Trans. Oncology* **2015**, *8*, 295–307, doi: 10.1016/j.tranon.2015.06.002.
 - (32) Bouclier, C.; Simon, M.; Laconde, G.; Pellerano, M.; Diot, S.; Lantuejoul, S.; Busser, B.; Vanwonterghem, L.; Vollaie, J.; Jossierand, V.; et al. Stapled peptide targeting the CDK4/Cyclin D interface combined with Abemaciclib inhibits KRAS mutant lung cancer growth. *Theranostics* **2020**, *10*, 2008–2028, doi:10.7150/thno.40971.
 - (33) Haines, E.; Chen, T.; Kommajosyula, N.; Chen, Z.; Herter-Sprie, G.S.; Cornell, L.; Wong, K.K.; Shapiro, G.I. Palbociclib resistance confers dependence on an FGFR-MAP kinase-mTOR-driven pathway in KRAS-mutant non-small cell lung cancer. *Oncotarget* **2018**, *9*, 31572–31589, doi:10.18632/oncotarget.25803.
 - (34) Herrera-Abreu, M.T.; Palafox, M.; Asghar, U.; Rivas, M.A.; Cutts, R.J.; Garcia-Murillas, I.; Pearson, A.; Guzman, M.; Rodriguez, O.; Grueso, J.; et al. Early adaptation and acquired resistance to CDK4/6 inhibition in estrogen receptor-positive breast cancer. *Cancer Res.* **2016**, *76*, 2301–2313, doi:10.1158/0008-5472.CAN-15-0728.

- (35) Cohen, P.; Alessi, D.R. Kinase Drug Discovery – What’s Next in the Field? *ACS Chem Biol* **2013**, *8*, 96–104, doi: 10.1021/cb300610s. Epub 2012 Dec 31
- (36) Guarnera, E.; Berezovsky, I. N. Allosteric sites: remote control in regulation of protein activity. *Curr.Opin.Struct.Biol.* **2016**, *37*, 1-8, doi: 10.1016/j.sbi.2015.10.004.
- (37) Tong, M.; Seeliger, M.A. Targeting conformational plasticity of protein kinases. *ACS Chem.Biol.* **2015**, *10*, 190–200, doi: 10.1021/cb500870a. Epub 2014 Dec 19
- (38) Leroux, A.E.; Biondi, R.M. Renaissance of Allostery to Disrupt Protein Kinase Interactions. *Trends Biochem.Sci.* **2020**, *45*, 27–41, doi: 10.1016/j.tibs.2019.09.007.

Treatments	24h	48h	72h
Roscovitine	31,8 ± 6,1	47,3 ± 6,8	50,5 ± 9
Roscovitine_Seq	29,6 ± 14	69,7 ± 14,9	73,7 ± 12,2
Ethaverine	28,3 ± 5,8	39,5 ± 9,5	50,2 ± 8,6
Ethaverine_Seq	29,1 ± 11,3	48,6 ± 14,5	60,2 ± 10,5
Papaverine	27,4 ± 7	33,0 ± 11,4	40,9 ± 10,2
Papaverine_Seq	26,0 ± 15,3	46,4 ± 12,6	41,4 ± 13,4
Rosco-Etha	48,3 ± 5,3	77,1 ± 10,2	87,5 ± 8,4
Rosco-Etha_Seq	43,8 ± 7,4	85,3 ± 4,3	92,3 ± 8,6
Rosco-Papa	44,6 ± 6	72,8 ± 9,9	81,6 ± 11,4
Rosco-Papa_Seq	38,6 ± 6	83,5 ± 5,2	89,7 ± 3,2

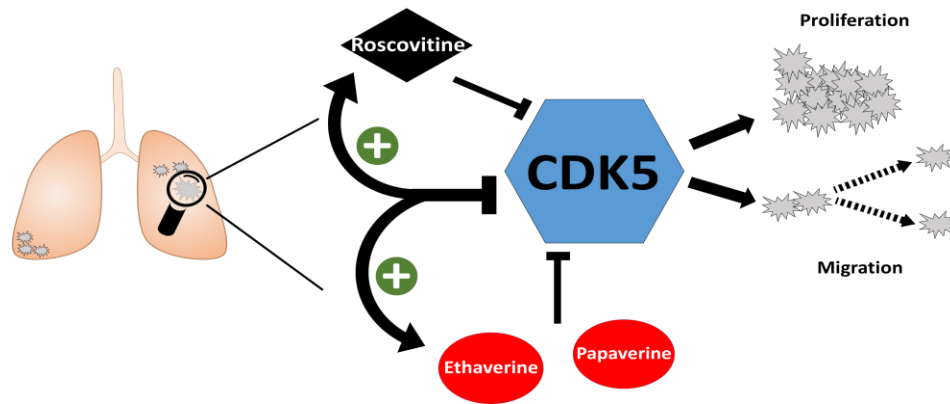
Table 1. Relative inhibition of A549 cells 24h, 48h, 72h after treatment. A549 cells were treated once with 9 µM Roscovitine, 11µM Ethaverine or 8µM Papaverine alone, or with combinations of 9 µM Roscovitine/11µM Ethaverine (Rosco-Etha) or 9 µM Roscovitine/8µM Papaverine (Rosco-Papa), or treated sequentially (“_Seq”) every 24h hours with each compound or the combinations. % cell inhibition relative to the mock are represented as mean ± SEM.

Cell line	Treatments	24h	48h	72h
H1299	Roscovitine	14,4 ± 12,3	26,5 ± 7,2	32,4 ± 8,7
	Ethaverine	31,6 ± 12,4	40,7 ± 8,4	49,4 ± 9,2
	Papaverine	29,3 ± 13,9	34,5 ± 9,3	43,5 ± 8,7
	Rosco-Etha	36,4 ± 11,3	60,9 ± 7,3	75,5 ± 5,3
	Rosco-Papa	34,5 ± 13,8	56,3 ± 2,9	72,2 ± 6,7
PC9	Roscovitine	22,9 ± 12	27,9 ± 14,1	14,2 ± 6,3
	Ethaverine	40,1 ± 12,1	48,1 ± 4,8	40,3 ± 5,7
	Papaverine	34,7 ± 14,1	32,0 ± 6,6	18,7 ± 4,2
	Rosco-Etha	45,4 ± 15	69,0 ± 5,1	72,3 ± 5,3
	Rosco-Papa	41,1 ± 17,2	62,2 ± 21,5	61,4 ± 9,8

Table 2. Relative inhibition of H1299 and PC9 cells 24h, 48h, 72h after treatment. H1299 and PC9 cells were treated with 9 µM Roscovitine, 11µM Ethaverine or 8µM Papaverine alone or with combinations of 9 µM Roscovitine/11µM Ethaverine (Rosco-Etha) or 9 µM Roscovitine/8µM Papaverine (Rosco-Papa). % cell inhibition relative to the mock Data are represented as mean ± SEM.

Treatments	24h	48h	72h
siRNA 1	25,7± 3	19,3± 0.7	---
siRNA 1+2	---	51,1± 1.7	---
siRNA 1+2+3	---	---	62,2
Rosco/Etha	---	28,3 ± 1.7	66,2 ± 1.5
siRNA 1 + Rosco/Etha	---	44.6 ± 0.7	---
siRNA 1 + 2 + Rosco/Etha	---	42,0± 5.2	---
siRNA 1 + 2 + 3	---	---	62,1± 5.1
siRNA 1 + 2 + 3 + Rosco/Etha	---	---	66 ± 2.7

Table 3. (see Figure 4). Relative inhibition of A549 cells treated with siRNA alone or combined with Roscovitine/Ethaverine. A549 cells were treated with 100nM siRNA 24h after seeding, then again 24h and 48h later alone or combined with Roscovitine/Ethaverine. % cell inhibition relative to the mock, measured 24h and 48h after inhibitor treatment are represented as mean ± SEM.



Ethaverine and Papaverine target CDK5 and inhibit lung cancer cell proliferation and migration.

Arthur Laure¹, Chloé Royet¹, Frederic Bihel², Blandine Baratte^{3,4}, Stéphane Bach^{3,4,5}, Marion Peyressatre¹ and May C. Morris^{1,*}

CDK5 kinase is dysregulated in lung cancer and constitutes an attractive pharmacological target. ATP-competitive inhibitors targeting CDK5 are poorly selective and suffer limitations, calling for new classes of inhibitors. In a screen for allosteric modulators of CDK5 we identified Ethaverine and closely related derivative Papaverine and showed that they inhibit cell proliferation and migration of non-small cell lung cancer cell lines. Moreover, their efficacy is significantly enhanced when combined with the ATP-competitive inhibitor Roscovitine, suggesting an additive, dual mechanism of inhibition targeting CDK5.
